


## Article

# Vegetation Restoration with Mixed N<sub>2</sub>-Fixer Tree Species Alleviates Microbial C and N Limitation in Surface Soil Aggregates in South Subtropical Karst Area, China

Xiaoyan Su <sup>1,†</sup>, Guannv Gao <sup>1,†</sup>, Xueman Huang <sup>1,2</sup>, Yi Wang <sup>3</sup>, Wen Zhang <sup>1</sup>, Jinliu Yan <sup>1</sup>, Weijun Shen <sup>1,2</sup>   
and Yeming You <sup>1,2,\*</sup>

<sup>1</sup> Guangxi Key Laboratory of Forest Ecology and Conservation, State Key Laboratory for Conservation and Utilization of Subtropical Agro-Bioresources, College of Forestry, Guangxi University, Nanning 530004, China

<sup>2</sup> Guangxi Youyiguan Forest Ecosystem Research Station, Pingxiang 532600, China

<sup>3</sup> Institute of Resources and Environment, International Centre for Bamboo and Rattan, Key Laboratory of National Forestry and Grassland Administration, Beijing for Bamboo & Rattan Science and Technology, Beijing 100102, China

\* Correspondence: youyeming@gxu.edu.cn; Tel.: +86-771-3271858

† These authors contributed equally to this work.



**Citation:** Su, X.; Gao, G.; Huang, X.; Wang, Y.; Zhang, W.; Yan, J.; Shen, W.; You, Y. Vegetation Restoration with Mixed N<sub>2</sub>-Fixer Tree Species Alleviates Microbial C and N Limitation in Surface Soil Aggregates in South Subtropical Karst Area, China. *Forests* **2022**, *13*, 1701. <https://doi.org/10.3390/f13101701>

Academic Editor: Manuel Esteban Lucas-Borja

Received: 20 September 2022

Accepted: 10 October 2022

Published: 16 October 2022

**Publisher's Note:** MDPI stays neutral with regard to jurisdictional claims in published maps and institutional affiliations.



**Copyright:** © 2022 by the authors. Licensee MDPI, Basel, Switzerland. This article is an open access article distributed under the terms and conditions of the Creative Commons Attribution (CC BY) license (<https://creativecommons.org/licenses/by/4.0/>).

**Abstract:** Soil extracellular enzyme stoichiometry (EES) is the essential predictor in nutrient status and resource limitation of soil microorganisms, whose metabolism has a vital role in biogeochemical cycling and ecosystem function. However, little is known about how N<sub>2</sub>-fixer tree species with different planting patterns affect soil nutrient resources in terms of extracellular enzyme activity (EEA) or EES within aggregates in degraded karst ecosystems. In this study, we evaluated soil EEA and EES related to carbon (C), nitrogen (N), and phosphorus (P) cycles across two eight-year-old pure plantations of legume species [*Dalbergia odorifera* T. Chen (PD) and *Acrocarpus fraxinifolius* Wight ex Arn. (PA)] and a mixed plantation of the two tree species listed above (MP). Meanwhile, a nearby undisturbed shrubland was used as a control (CK). We concluded that the activities of C-, N-, and P-acquiring enzyme increased to different degrees in the N<sub>2</sub>-fixer tree species stands (particularly in MP) compared to CK in all aggregates. Compared to CK, MP significantly increased by 39.0%, 54.0%, 39.3%, and 24.8% in total C-acquiring EEA, 41.1%, 60.5%, 47.8%, and 12.5% in total N-acquiring EEA, and 100.4%, 79.7%, 69.2%, and 56.4% in total P-acquiring EEA within >2 mm, 1–2 mm, 0.25–1 mm, and <0.25 mm aggregates, respectively. Furthermore, the logarithmic transformed ratio of C-, N-, and P-acquiring enzyme activities was 1.20:1.08:1, which deviated from the global ratio (1:1:1). Vector analysis of EEA showed that the vector length (VL) within aggregates was significantly lower than that of CK in all stands of N<sub>2</sub>-fixer species except PD; while in all treatments, vector angle (VA) was <45° for all aggregate sizes, except in MP, where VA reached 45° for <0.25 mm aggregate. These indicated soil microbes were limited by C and N together. However, MP significantly alleviated microbial C and N limitation than CK ( $p < 0.05$ ). There were obvious positive relationships between enzyme C:N, C:P, and N:P ratios. VL was markedly negatively linked to VA. EES was markedly related to most soil nutrients and microbial biomass stoichiometry ratios. Changes in soil EEA and EES were primarily driven by available phosphorus (AP), microbial biomass carbon (MBC), soil C:N and MBN:MBP ratios. Together, our results demonstrate the influences after introducing N<sub>2</sub>-fixer tree species (particularly MP) for vegetation recovery on soil microbial nutrient limitation and ecological processes in aggregate level and will contribute to the development of ecological restoration practices and fertility management in degraded karst ecosystems of southwest China.

**Keywords:** enzyme activity; enzyme stoichiometry; karst ecosystem; N<sub>2</sub>-fixer tree species; nutrient limitation; soil aggregates

## 1. Introduction

Soil extracellular enzymes are metabolites mainly generated by plant roots and microorganisms that contribute to the decomposition and transformation of plant residual materials and perform important roles in the material circulation and energy flow of ecosystems [1,2]. Therefore, the extracellular enzyme activity (EEA) is often used as a sensitive predictor of soil productivity and nutrient status [3,4]. Soil extracellular enzyme stoichiometry (EES), which is the proportion of EEA, captures nutrient acquisition of microbes and the availability of limited resources [5–7]. Several previous works have studied EES and soil carbon (C), nitrogen (N), and/or phosphorus (P) cycles and their links to soil nutrient and microbial biomass stoichiometry to better reflect the dynamic balance between microbial nutrient demand and growth metabolism [8–10]. EEA and EES are strongly dependent on microbial biomass and composition [11] and environmental conditions, i.e., climate [12] and soil properties [13], particularly soil organic carbon (SOC), total nitrogen (TN), and soil pH [11,14,15]. Variations in plant types can trigger differences of fine roots [16], litter qualities [17], MBC [15], and soil physiochemical properties [18,19], and thus influence soil EEA in turn. Nevertheless, these drivers were not consistent in their effects on soil EEA and EES across ecosystems. Hence, it is essential to illuminate the main drivers that lead to microbial resource limitations for different vegetation types and at regional scales.

Being the fundamental unit of soil physical structure, aggregates are the dominant factor affecting pore characteristics [20] and mechanical resistance [21], and eventually water and nutrient retention [22,23]. Soil aggregates are typically divided into macro (>0.25 mm) and micro-aggregates (<0.25 mm) [24]. Soil aggregates not only served as predictors of microbial biomass, microbial community composition, and EEA but also directly influenced the dynamic balance of soil microbial communities and thus EEA [25,26]. Land use/cover changes such as reforestation, afforestation, and vegetation succession, can alter key soil physiochemical properties including SOC, TN, and mean weight diameter (MWD) of aggregates, which greatly affect soil fertility [27]. Therefore, studies addressing soil aggregate and associated EEA, and EES are of great significance for understanding changes in soil nutrients and ground strength maintenance capacity.

Karst landscapes are mostly based on limestone or dolomite, where the topography is formulated by dissolving rock [28,29]. Karst landscapes account for approximately 15% of the global land area; the largest karst ecosystem worldwide is in southwest China, with an area of ~550,000 km<sup>2</sup> [30]. Large karst regions in southwest China have experienced severe deforestation due to human disturbances, particularly intensive agricultural activity [31]. In recovering karst ecosystems, soil nutrients are mainly characterized by N restriction during the pre-recovery period, P restriction during the late successional period, and combined N and P limitation in the mid-recovery period [32,33]. Natural vegetation restoration and artificial afforestation are the best methods for managing rock desertification, and suitable tree species and stand types must be selected to obtain better ecological restoration effects in degraded karst ecosystems [34,35]. For example, N<sub>2</sub>-fixer plants can improve the effectiveness of soil N, thereby accelerating the restoration of degraded karst ecosystems [36,37]. In addition, mixed plantations obviously change the stand structure compared to pure plantations, creating conditions for other plants to grow and increasing biodiversity, which plays an important role in maintaining and enhancing the stability of forest ecosystems [38,39]. Several studies have examined the associations between microbial communities, EEA, and C, N, and P cycles on karst region surface soils [40–42]. In a previous study, we found that introducing one or two N<sub>2</sub>-fixer tree species in a karst area altered surface soil physiochemical properties and microbial community structure to different degrees; notably, the mixed stand of two N<sub>2</sub>-fixer tree species markedly improved the accumulation and effectiveness of soil organic P [43]. These findings indicated that N<sub>2</sub>-fixed tree species can be available to improve the recovery of accelerated degraded karst ecosystems, as they can add N input through fixation of atmospheric N. However, the influences after introducing N<sub>2</sub>-fixer tree species on aggregate nutrient limitations of soils, particularly C, N, and P limitation, remain unclear. Furthermore, prior research

about nutrient limitations had mainly concentrated on vegetation biomass, foliage, or soil stoichiometry, rather than soil aggregates.

In our research, we evaluated the influences of N<sub>2</sub>-fixer tree species on the soil EEA of C-, N-, and P-acquiring and microbial nutrient limitations according to various planting patterns with different soil physicochemical and biotic characteristics in a degraded karst ecosystem. We hypothesized that (1) the EEA and EES of soil aggregates were substantially affected by introduction of N<sub>2</sub>-fixer tree species; (2) the changes of soil EEA and EES may be explained by the variations in soil physicochemical and microbial properties. The major objectives of our research, therefore, were to (1) estimate the changes of EEA and EES in soil aggregates under two N<sub>2</sub>-fixer tree species restoration patterns (one or mixed two tree species) and (2) reveal relative microbial resource limitations and identify the crucial factors influencing the soil EEA and EES parameters.

## 2. Materials and Methods

### 2.1. Site Description

The sites used in our study were located in Mashan County (23°24′–24°20′ N, 107°41′–108°29′ E), in the north-central Guangxi Zhuang Autonomous Region, China. The study area has a southern subtropical monsoon climate, with mean annual temperature and rainfall of 21.3 °C and 1667.1 mm, respectively. The study site features a well-developed karst landscape, and the soil texture is mainly limestone soil formed by carbonatites, with shallow soil layer, highly stony particles, heavy clay texture, weak alkaline soil pH, and large slope, usually above 25°. Due to the long-term activities of local residents such as deforestation, grazing, and reclamation agriculture, this area has experienced serious soil erosion, fragmentation, and rock exposure, producing a fragile ecological environment with severe stone desertification. Since 2002, when China implemented the “Grain for Green” project, the region has been gradually restored from abandoned farmland to natural vegetation.

### 2.2. Experimental Design and Sample Collection

In March 2011, we set up a completely randomized block design with five experimental blocks (~6 hm<sup>2</sup>) containing four different treatments. The experimental design and basic information for the sample sites are described in detail in Li et al. [43]. Briefly, the four treatments included pure plantations of the precious timber tree species *Dalbergia odorifera* (Leguminosae) (PD); pure plantations of the fast-growing tree species *Acrocarpus fraxinifolius* (Leguminosae), which is usually applied to afforestation in karst areas (PA); and mixed plantations of the two tree species listed above, planted randomly at a 3:7 mixing ratio (MP). Adjacent shrublands naturally regenerated since 2002, without trees, were used as a control (CK). In August 2019, a 20 m × 20 m sampling site was set up to each experimental treatment within each block, considering variation in spatial representation and topography.

In each 20 m × 20 m plot, we randomly collected 10 soil samples (depth, 0–10 cm) and maintained their natural aggregates to the greatest extent possible. The samples were mixed into a sterile polypropylene bag, and the mixed soil samples were taken back to the lab, where contaminants, such as rocks and plant roots, were eliminated. Each mixed sample was carefully divided along the natural fragile surface and divided into two equivalent parts: one part was used for aggregate size separation, and the other was used to measure whole soil properties, including soil physicochemical properties, microbial biomass, and EEA (Table 1).

**Table 1.** Characteristics of the whole soil in four treatments (mean  $\pm$  standard error,  $n = 5$ ).

Treatment	CK	PD	PA	MP
SOM (g/kg)	39.75 $\pm$ 4.49 b	61.11 $\pm$ 5.48 a	61.03 $\pm$ 4.55 a	69.59 $\pm$ 6.57 a
TN (g/kg)	4.49 $\pm$ 0.88 a	4.29 $\pm$ 0.33 a	4.65 $\pm$ 0.56 a	4.26 $\pm$ 0.49 a
TP (g/kg)	0.25 $\pm$ 0.08 a	0.28 $\pm$ 0.05 a	0.28 $\pm$ 0.04 a	0.23 $\pm$ 0.08 a
NH <sub>4</sub> <sup>+</sup> -N (mg/kg)	14.25 $\pm$ 1.06 a	18.38 $\pm$ 2.30 a	15.93 $\pm$ 1.42 a	14.92 $\pm$ 1.76 a
NO <sub>3</sub> <sup>-</sup> -N (mg/kg)	19.28 $\pm$ 2.09 b	19.39 $\pm$ 0.81 b	28.18 $\pm$ 2.52 ab	34.17 $\pm$ 3.67 a
AP (mg/kg)	6.56 $\pm$ 0.63 c	7.07 $\pm$ 0.70 c	11.10 $\pm$ 1.26 b	18.01 $\pm$ 0.64 a
pH	7.65 $\pm$ 0.05 a	7.49 $\pm$ 0.07 a	7.63 $\pm$ 0.07 a	7.02 $\pm$ 0.25 a
MBC (mg/kg)	108.38 $\pm$ 9.11 b	121.28 $\pm$ 7.93 b	158.02 $\pm$ 16.15 a	160.91 $\pm$ 11.85 a
MBN (mg/kg)	20.60 $\pm$ 1.28 b	21.10 $\pm$ 1.65 b	23.83 $\pm$ 1.08 ab	29.69 $\pm$ 1.23 a
MBP (mg/kg)	12.70 $\pm$ 1.03 b	13.99 $\pm$ 1.63 b	17.26 $\pm$ 1.92 ab	22.47 $\pm$ 2.69 a
BG + CB + XYL (nmol·g <sup>-1</sup> ·h <sup>-1</sup> )	600.83 $\pm$ 15.05 c	695.17 $\pm$ 13.08 b	733.87 $\pm$ 15.40 b	795.87 $\pm$ 17.05 a
LAP + NAG (nmol·g <sup>-1</sup> ·h <sup>-1</sup> )	312.50 $\pm$ 11.60 c	357.66 $\pm$ 9.76 b	386.53 $\pm$ 9.60 b	418.32 $\pm$ 10.42 a
ALP (nmol·g <sup>-1</sup> ·h <sup>-1</sup> )	184.51 $\pm$ 5.47 b	194.39 $\pm$ 4.29 b	257.83 $\pm$ 12.10 a	255.70 $\pm$ 14.19 a
VL	1.66 $\pm$ 0.01 a	1.66 $\pm$ 0.00 a	1.62 $\pm$ 0.01 b	1.64 $\pm$ 0.00 b
VA (°)	42.18 $\pm$ 0.14 b	41.87 $\pm$ 0.11 b	42.98 $\pm$ 0.12 a	42.68 $\pm$ 0.11 a
MWD (mm)	2.95 $\pm$ 0.10 b	2.98 $\pm$ 0.20 b	3.01 $\pm$ 0.10 b	3.15 $\pm$ 0.20 a

Note: SOM, soil organic matter; TN, total nitrogen; TP, total phosphorus; NH<sub>4</sub><sup>+</sup>-N, ammonium nitrogen; NO<sub>3</sub><sup>-</sup>-N, nitrate nitrogen; AP, available phosphorus; pH, pH value; MBC, microbial biomass carbon; MBN, microbial biomass nitrogen; MBP, microbial biomass phosphorus; BG + CB + XYL, total C-acquiring enzyme activity ( $\beta$ -1,4-glucosidase and  $\beta$ -D-Cellobiosidase and  $\beta$ -1,4-xylosidase); LAP + NAG, total N-acquiring enzyme activity ( $\beta$ -1,4-N-acetylglucosaminidase and L-leucine aminopeptidase); ALP, total P-acquiring enzyme activity (alkaline phosphatase); VL, vector length; VA, vector angle; MWD, mean weight diameter. Different lowercase letters within the same row indicate significant differences ( $p < 0.05$ ) among treatments.

### 2.3. Soil Aggregate Separation

Separation of soil aggregates was conducted using the dry sieving method, which was demonstrated in the study of Schutter and Dick [44]. Briefly, the fresh soils were cooled and dried at 4 °C till the gravimetric water content with approximately 80 g H<sub>2</sub>O per kg was obtained and the disturbance was minimized to microbial communities. The aggregates were passed through soil sieves (mesh sizes, 4.76, 2.0, 1.0, and 0.25 mm) to divide them into four fractions: >2 mm, 1–2 mm, 0.25–1 mm, and <0.25 mm. Finally, soil physicochemical and microbial characteristics and EEA values were measured within each aggregate size (Table S1).

### 2.4. Soil Physicochemical Properties and Microbial Biomass Analysis

The aggregate proportion of each diameter class was measured by dry-sieving, and the MWD was used to evaluate aggregate stability [45]. Soil pH was tested by pH meter (1:2.5 soil: water proportion); SOC was measured with K<sub>2</sub>Cr<sub>2</sub>O<sub>7</sub>-H<sub>2</sub>SO<sub>4</sub> oxidation method. TN was conducted by semi-micro Kjeldahl digestion [46]. The ammonium N (NH<sub>4</sub><sup>+</sup>-N) and nitrate N (NO<sub>3</sub><sup>-</sup>-N) concentrations were analyzed using CaCl<sub>2</sub> (0.01 mol/L) extraction and AutoAnalyzer III (SEAL Analytical, Norderstedt, Germany). Total P (TP) was extracted by H<sub>2</sub>SO<sub>4</sub>-HClO<sub>7</sub> ablation, and the content of P in the extracting solution was estimated using the molybdenum blue colorimetric technology [47]. Available P (AP) was abstracted using 0.5 mol/L NaHCO<sub>3</sub> (pH = 8.5), and the content was estimated by the molybdenum blue colorimetric method [47,48]. Microbial biomass nitrogen (MBN), phosphorus (MBP), and MBC were tested via the chloroform fumigation-extraction technology [49–51].

### 2.5. Soil EEA and EES Analysis

The activities of soil C- ( $\beta$ -1,4-glucosidase [BG],  $\beta$ -D-cellobiosidase [CB] and  $\beta$ -1,4-xylosidase [XYL]), N- ( $\beta$ -N-acetylglucosaminidase [NAG] and leucine aminopeptidase [LAP]), and P-acquiring enzymes (alkaline phosphatase [ALP]) were measured by a 96-microplate fluorescence method. Detailed description about the technologies were displayed by Saiya-Cork et al. [52]. Information on C-, N-, and P-acquiring enzymes and their corresponding substrates is provided in Table S2. Soil EEA was expressed as nmol g<sup>-1</sup> h<sup>-1</sup>,

and EES was computed as the proportion of C-, N-, and P-acquiring EEA [7,53,54], as follows:

$$\text{Soil enzyme C:N ratio} = \ln(\text{BG} + \text{CB} + \text{XYL}) : \ln(\text{LAP} + \text{NAG}) \quad (1)$$

$$\text{Soil enzyme C:P ratio} = \ln(\text{BG} + \text{CB} + \text{XYL}) : \ln(\text{ALP}) \quad (2)$$

$$\text{Soil enzyme N:P ratio} = \ln(\text{LAP} + \text{NAG}) : \ln(\text{ALP}) \quad (3)$$

## 2.6. Calculation and Statistical Analysis

Mean weight diameter (MWD, mm), which was applied to assess aggregate stability, was calculated as described by Fattet et al. [55], as follows:

$$MWD = \sum_{i=1}^n (X_i \times W_i) \quad (4)$$

where in  $X_i$  is the average diameter of size fraction  $i$  (mm),  $W_i$  is the percent of each size fraction within whole soil sample (%).

Vector analysis of soil EEA can be applied to characterize the relative limitation status of soil microorganisms by C, N, or P [56]. The vector length (VL) and vector angle (VA) are computed as follows [10]:

$$VL = SQRT \left\{ \left[ \frac{\ln(\text{BG} + \text{CB} + \text{XYL})}{\ln(\text{LAP} + \text{NAG})} \right]^2 + \left[ \frac{\ln(\text{BG} + \text{CB} + \text{XYL})}{\ln(\text{ALP})} \right]^2 \right\} \quad (5)$$

$$VA = \text{Degrees} \left\{ \text{ATAN2} \left[ \left( \frac{\ln(\text{BG} + \text{CB} + \text{XYL})}{\ln(\text{ALP})} \right), \left( \frac{\ln(\text{BG} + \text{CB} + \text{XYL})}{\ln(\text{LAP} + \text{NAG})} \right) \right] \right\} \quad (6)$$

where *SQRT* is the open-square operator function, *Degrees* is the angle conversion function, and *ATAN2* is the inverse tangent function. Longer *VL* indicates that microorganisms are more restricted by C, and  $VA < 45^\circ$  and  $VA > 45^\circ$  indicate that microorganisms are restricted by N and P, respectively [56].

The relative enzyme activity index (REAI) and relative enzyme activity comprehensive index (REACI) can be used to express the protective effect of soil aggregates on EEA; they are calculated as follows:

$$REAI = EA_i / EA_s \quad (7)$$

$$REACI = (REAI_C + REAI_N + REAI_P) / 3 \quad (8)$$

where  $EA_i$  denotes enzyme activity in the  $i$ th size aggregate, and  $EA_s$  denotes the whole-soil enzyme activity.  $REAI_C$ ,  $REAI_N$ , and  $REAI_P$  are the relative activity indexes of soil C-, N-, and P-acquiring enzymes, respectively.

The normality of the data distribution was checked for homogeneity prior to statistical analysis. Data analysis was conducted by the SPSS 25.0 software. All findings are exhibited as means  $\pm$  standard error. One-way ANOVA was conducted to assess the influences of various treatments (CK, PD, PA, or MP) on indicators of soil C-, N-, and P-acquiring EEA, EES, VL, VA, and relative activity indexes of C-, N-, and P-acquiring enzymes. The influences of treatment and aggregate size and their associations on soil EEA and EES, VL, and VA, and relative activity indexes of C-, N-, and P-acquiring enzymes were investigated using two-way ANOVA. Significant differences were evaluated at a level of  $p < 0.05$ . Pearson correlation analysis was conducted to assess the relationships among nutrient and microbial biomass stoichiometry ratios and soil EES.

Variance-partitioning analysis (VPA) was undertaken to determine the comparative significances about two categories of predictors, soil physicochemical characteristics (SOC; TN; TP; pH; MWD; soil C:N, C:P, and N:P ratios; AP;  $\text{NO}_3\text{-N}$ ;  $\text{NH}_4^+\text{-N}$ ) and microbial properties (MBC; MBN; MBP; MBC:MBN, MBC:MBP, and MBN:MBP ratios) on soil EEA and EES related to microbial C, N, and P metabolism; and the results were represented in the Venn diagrams. Meanwhile, we use the redundancy analysis (RDA) to confirm which

soil physicochemical and microbial characteristics were most associated with soil EEA and EES. An artificial forward selection method was used in RDA to assess the importance ( $p < 0.05$ ) and order of influence by each factor on EEA and EES by Monte Carlo test (499 permutations). VPA and RDA were conducted in CANOCO 5.0 software. All data were log transformed previously to statistical analysis [57].

We selected significant environmental variables from the results of the Pearson correlation analysis and RDA and divided them into four categories: soil nutrient, microbial biomass, nutrient stoichiometry, and microbial biomass stoichiometry. Then, structural equation modeling (SEM) was forward conducted to determine the influences from various characteristics on EEA and EES either directly or indirectly, and thus the nutrient resource limitation status of microbial metabolism. The model was constructed using AMOS 26.0 software.

### 3. Results

#### 3.1. Influences of Different Treatments on Soil EEA within Aggregates

Treatment and aggregate size had significant main and interactive influences on the total activities of soil C-, N-, and P-acquiring enzyme ( $p < 0.01$ ; Figure 1). The total activity of C-acquiring enzyme in MP was significantly higher than those in PD, PA, and CK for all aggregate sizes ( $p < 0.05$ ). Specifically, compared to CK, MP significantly increased by 39.0%, 54.0%, 29.3%, and 24.8% in  $>2$ , 1–2, 0.25–1, and  $<0.25$  mm aggregates, respectively. The PD and PA plots had markedly higher total C-acquiring EEA than CK in aggregates  $>2$ , 1–2, and 0.25–1 mm in size, while no obvious differences were discovered among the PD and PA plots in all aggregate fractions ( $p > 0.05$ ; Figure 1a). The trend in total N-acquiring EEA was similar to that of total C-acquiring EEA, and MP significantly increased by 41.1%, 60.5%, 47.8%, and 12.5% relative to CK in  $>2$ , 1–2, 0.25–1, and  $<0.25$  mm aggregates, respectively (Figure 1b). P-acquiring EEA was markedly higher in the MP and PA than in the CK and PD for  $>2$  mm aggregates ( $p < 0.05$ ), whereas for aggregates 1–2, 0.25–1, and  $<0.25$  mm in size, ALP of MP was markedly higher compared to CK, PD, and PA ( $p < 0.05$ ). The ALP in MP was increased by 100.4%, 79.7%, 69.2%, and 56.4% over CK in  $>2$ , 1–2, 0.25–1, and  $<0.25$  mm aggregates, respectively, but there were no obvious variations among PD, PA, and CK ( $p > 0.05$ ; Figure 1c).

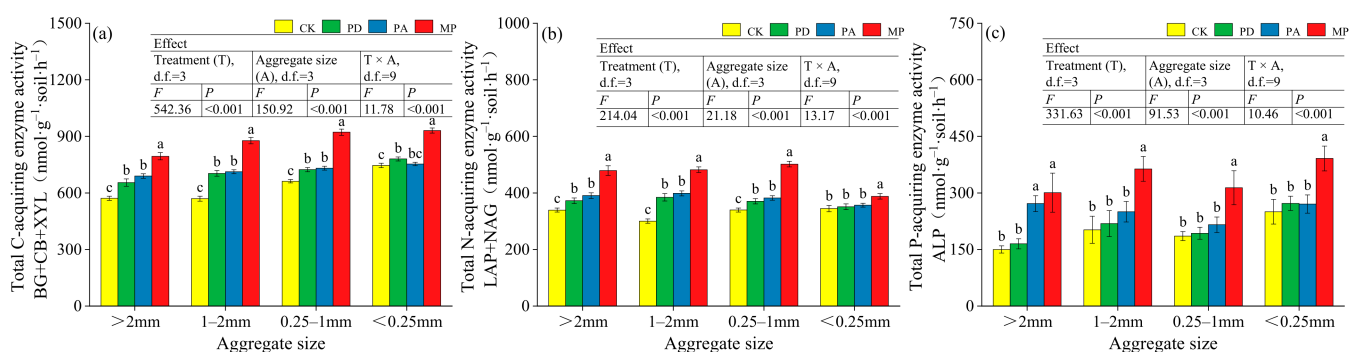


**Figure 1.** (a–c) Variations in C-, N-, and P-acquiring EEA within soil aggregates of different treatments. Different lowercase letters above the bars indicate significant differences ( $p < 0.05$ ) between treatments within the same soil aggregate fraction. Error bars indicate standard error ( $n = 5$ ).

There were obvious major and interactive influences of treatment and aggregate size on  $REAI_C$ ,  $REAI_N$ ,  $REAI_P$ , and  $REACI$  ( $p < 0.01$ ; Table 2). In all plots,  $REAI_C$  decreased significantly as the aggregate size increased, although  $REAI_N$  did not differ significantly among most aggregate sizes.  $REAI_P$  trends in CK, PD, and MP treatments were similar to those of  $REAI_C$ , and the  $REAI_P$  of MP was  $>1$  for all aggregate sizes. However, the  $REAI_P$  of PA was higher for aggregates  $>2$  and  $<0.25$  mm in size, and significantly lower for 0.25–1 mm aggregate ( $p < 0.05$ ). In contrast to the PA, PD, and CK stands, the  $REACI$  of

MP was >1 for all aggregate sizes. Importantly, the REACI was higher for small aggregates than for large aggregates in all plots (Table 2).

**Table 2.** Variations in the relative activity indexes of C-, N-, and P-acquiring enzymes within soil aggregates of different treatments (mean  $\pm$  standard error,  $n = 5$ ).

Treatment	Aggregate Size	REAI <sub>C</sub>		REAI <sub>N</sub>		REAI <sub>P</sub>		REACI	
CK	>2 mm	0.95 $\pm$ 0.03 c		1.09 $\pm$ 0.02 a		0.82 $\pm$ 0.04 c		0.95 $\pm$ 0.01 c	
	1–2 mm	0.95 $\pm$ 0.03 c		0.96 $\pm$ 0.03 b		1.10 $\pm$ 0.03 b		1.00 $\pm$ 0.02 c	
	0.25–1 mm	1.10 $\pm$ 0.03 b		1.09 $\pm$ 0.04 a		1.01 $\pm$ 0.04 b		1.07 $\pm$ 0.02 b	
	<0.25 mm	1.24 $\pm$ 0.04 a		1.11 $\pm$ 0.03 a		1.36 $\pm$ 0.05 a		1.24 $\pm$ 0.02 a	
PD	>2 mm	0.94 $\pm$ 0.03 c		1.04 $\pm$ 0.04 a		0.85 $\pm$ 0.04 c		0.95 $\pm$ 0.02 c	
	1–2 mm	1.01 $\pm$ 0.04 bc		1.08 $\pm$ 0.04 a		1.13 $\pm$ 0.03 b		1.07 $\pm$ 0.02 b	
	0.25–1 mm	1.04 $\pm$ 0.03 ab		1.04 $\pm$ 0.03 a		0.99 $\pm$ 0.03 b		1.03 $\pm$ 0.02 b	
	<0.25 mm	1.12 $\pm$ 0.03 a		0.98 $\pm$ 0.03 a		1.40 $\pm$ 0.06 a		1.17 $\pm$ 0.03 a	
PA	>2 mm	0.94 $\pm$ 0.01 b		1.01 $\pm$ 0.04 a		1.05 $\pm$ 0.02 a		1.00 $\pm$ 0.01 a	
	1–2 mm	0.97 $\pm$ 0.02 ab		1.03 $\pm$ 0.03 a		0.97 $\pm$ 0.04 a		0.99 $\pm$ 0.01 a	
	0.25–1 mm	1.00 $\pm$ 0.01 ab		0.99 $\pm$ 0.03 a		0.84 $\pm$ 0.02 b		0.94 $\pm$ 0.01 b	
	<0.25 mm	1.03 $\pm$ 0.03 a		0.96 $\pm$ 0.02 a		1.05 $\pm$ 0.03 a		1.01 $\pm$ 0.01 a	
MP	>2 mm	1.00 $\pm$ 0.03 b		1.14 $\pm$ 0.02 a		1.18 $\pm$ 0.04 c		1.11 $\pm$ 0.01 b	
	1–2 mm	1.10 $\pm$ 0.01 a		1.15 $\pm$ 0.03 a		1.39 $\pm$ 0.03 b		1.22 $\pm$ 0.01 a	
	0.25–1 mm	1.16 $\pm$ 0.04 a		1.19 $\pm$ 0.04 a		1.23 $\pm$ 0.03 c		1.19 $\pm$ 0.02 a	
	<0.25 mm	1.17 $\pm$ 0.03 a		0.95 $\pm$ 0.03 b		1.53 $\pm$ 0.03 a		1.22 $\pm$ 0.02 a	
Factor		<i>F</i>	<i>P</i>	<i>F</i>	<i>P</i>	<i>F</i>	<i>P</i>	<i>F</i>	<i>P</i>
Treatment (T), d.f. = 3		21.169	<0.001	11.347	<0.001	65.598	<0.001	100.768	<0.001
Aggregate size (A), d.f. = 3		49.081	<0.001	6.618	<0.01	75.476	<0.001	63.96	<0.001
T $\times$ A, d.f. = 9		4.881	<0.001	5.928	<0.001	8.482	<0.001	13.457	<0.001

Note: REAI<sub>C</sub>, relative activity index of soil C-acquiring enzyme; REAI<sub>N</sub>, relative activity index of soil N-acquiring enzyme; REAI<sub>P</sub>, relative activity index of P-acquiring enzyme; REACI, relative activity comprehensive index of soil enzymes. Different lowercase letters within the same column indicate significant differences ( $p < 0.05$ ) among soil aggregate fractions within the same treatment.

### 3.2. Influences of Different Treatments on Soil EES within Aggregates

There were highly significant main and interactive influences of treatment and aggregate size on soil enzyme C:P and N:P ratios ( $p < 0.001$ ; Figure 2b,c). However, enzyme C:N ratios varied markedly only among soil aggregate sizes, and a significant treatment  $\times$  aggregate size interactive influence was detected ( $p < 0.001$ ; Figure 2a). Notably, the enzyme C:N ratio was markedly lower in 1–2 and 0.25–1 mm aggregates but markedly higher within <0.25 mm aggregate, in MP than CK ( $p < 0.05$ ). The enzyme C:N ratio in PA and PD were not markedly different in all aggregates ( $p > 0.05$ ) except 1–2 mm aggregates, where they were markedly lower in PA than in CK ( $p < 0.05$ ; Figure 2a). The enzyme C:P and enzyme N:P ratios in MP and PA were markedly lower compared to PD and CK ( $p < 0.05$ ) among >2 mm aggregates, whereas there was no obvious variation between PD and CK ( $p > 0.05$ ). However, among in 1–2, 0.25–1, and <0.25 mm aggregates, MP had markedly lower enzyme C:P and enzyme N:P ratios compared to PA, PD, and CK ( $p < 0.05$ ), with no obvious variation between PA and either PD or CK ( $p > 0.05$ ; Figure 2b,c).

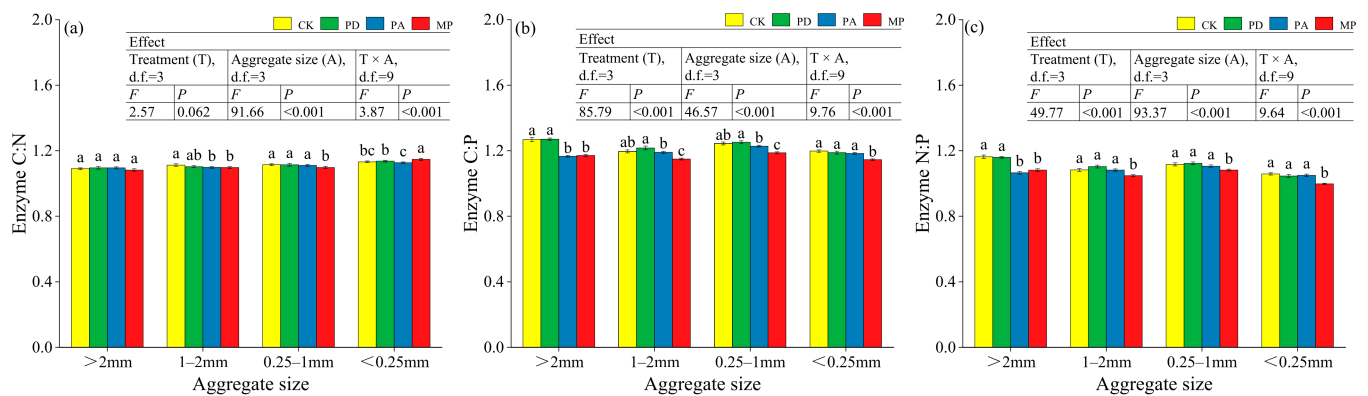


**Figure 2.** (a–c) Variations in C-, N-, and P-acquiring EES within soil aggregates of different treatments. Different lowercase letters above the bars indicate significant differences ( $p < 0.05$ ) between treatments within the same soil aggregate fraction. Error bars indicate standard error ( $n = 5$ ).

Treatment and aggregate size had obvious major and interactive influences on VL and VA ( $p < 0.001$ ; Figure 3a,b). In all stands, VL ranged from 1.589 to 1.678. VL was significantly lower in MP and PA than in PD and CK for  $>2$  mm aggregates ( $p < 0.05$ ). However, aggregates 1–2, 0.25–1, and  $<0.25$  mm in size had markedly lower VL in MP compared to PD and CK ( $p < 0.05$ ), and PA had lower VL than CK, whereas there was no obvious variation between PD and CK ( $p > 0.05$ ; Figure 3a). In all stands, VA was  $<45^\circ$  for all aggregate sizes, except in MP, where VA reached  $45^\circ$  for  $<0.25$  mm aggregates, indicating that microbial metabolism was mainly limited by soil N in all stands (Figure 3b). Notably, VA was markedly higher for MP and PA than for PD and CK in  $>2$  mm aggregates ( $p < 0.05$ ); VA was markedly higher for MP than for PA, PD, and CK for 1–2, 0.25–1, and  $<0.25$  mm aggregates ( $p < 0.05$ ), and there were no obvious variations between PA, PD, and CK ( $p > 0.05$ ; Figure 3b). Thus, soil microorganisms were less affected by C and N limitation in MP than in CK.

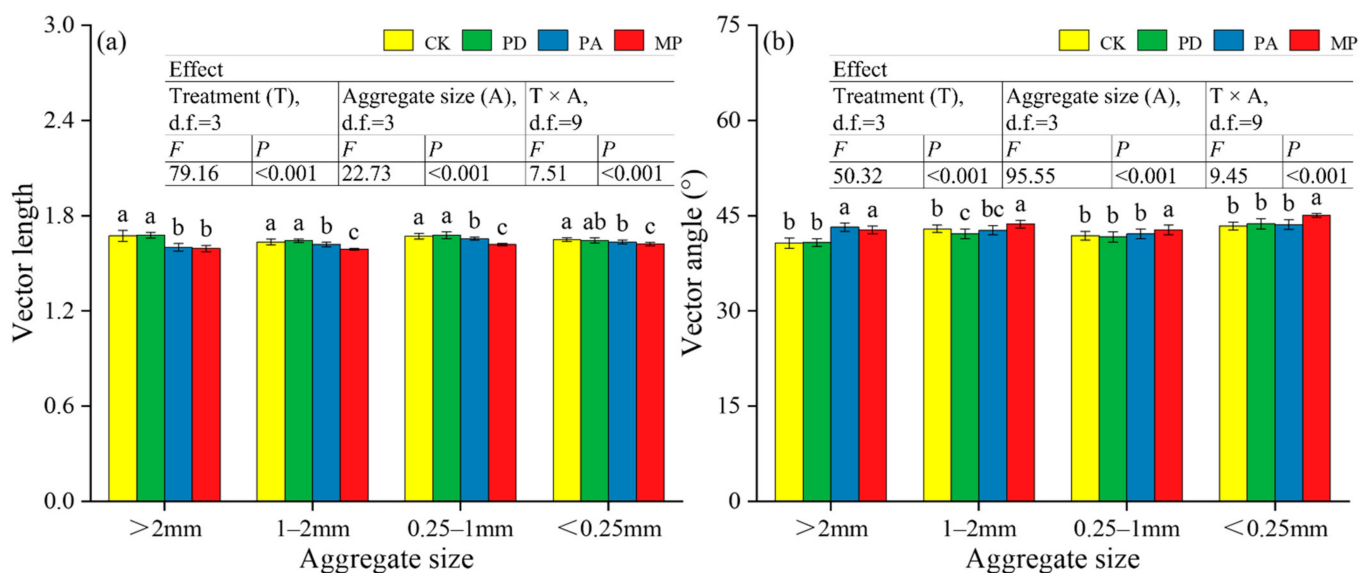
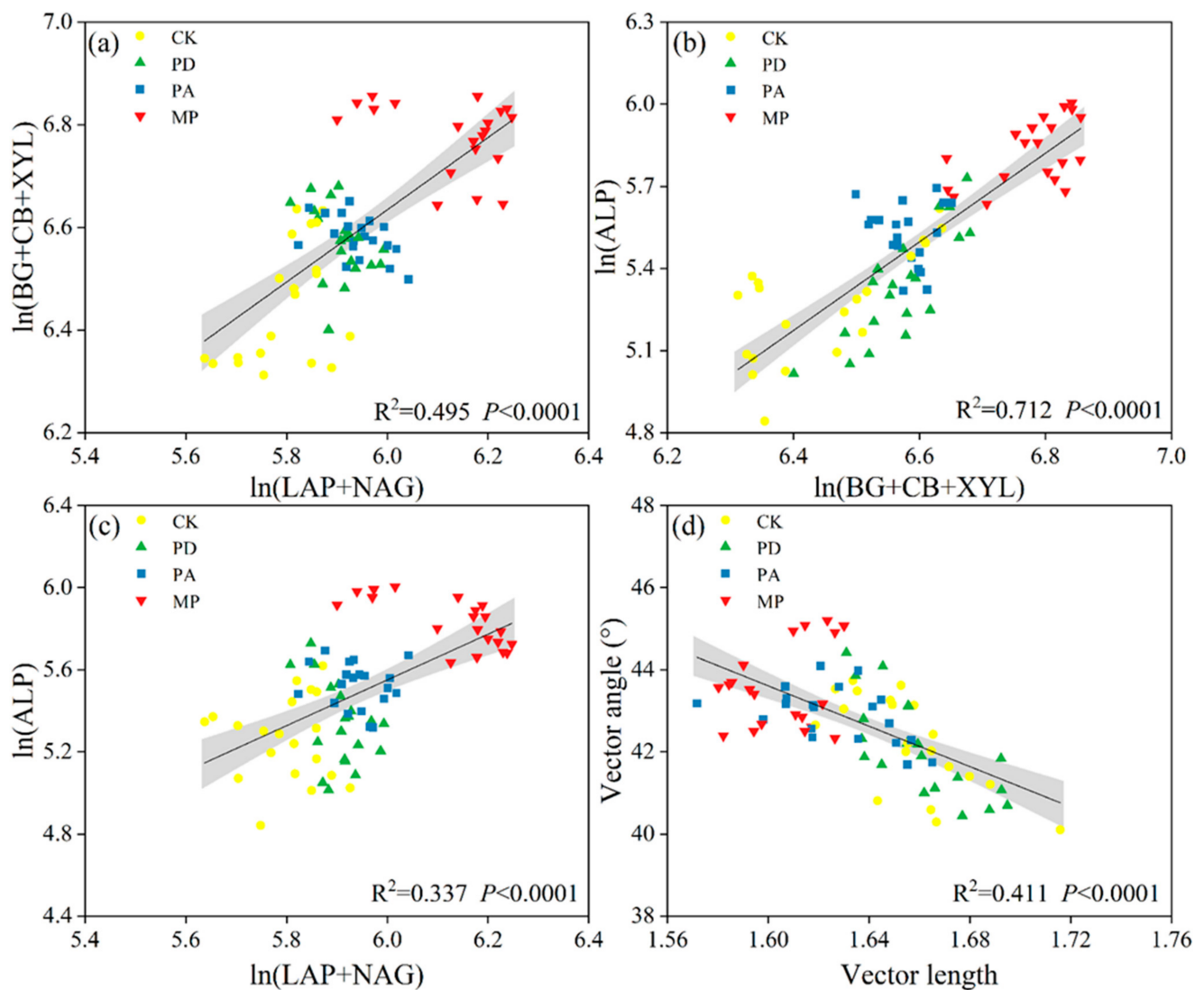


**Figure 3.** (a,b) Vector analysis of C-, N-, and P-acquiring EEA within soil aggregates on different treatments. Different lowercase letters above the bars indicate significant differences ( $p < 0.05$ ) between treatments within the same soil aggregate fraction. Error bars indicate standard error ( $n = 5$ ).

Linear regression analysis suggested that total C-, N-, and P-acquiring enzyme activities were highly markedly positively correlated among different treatments ( $p < 0.0001$ ;

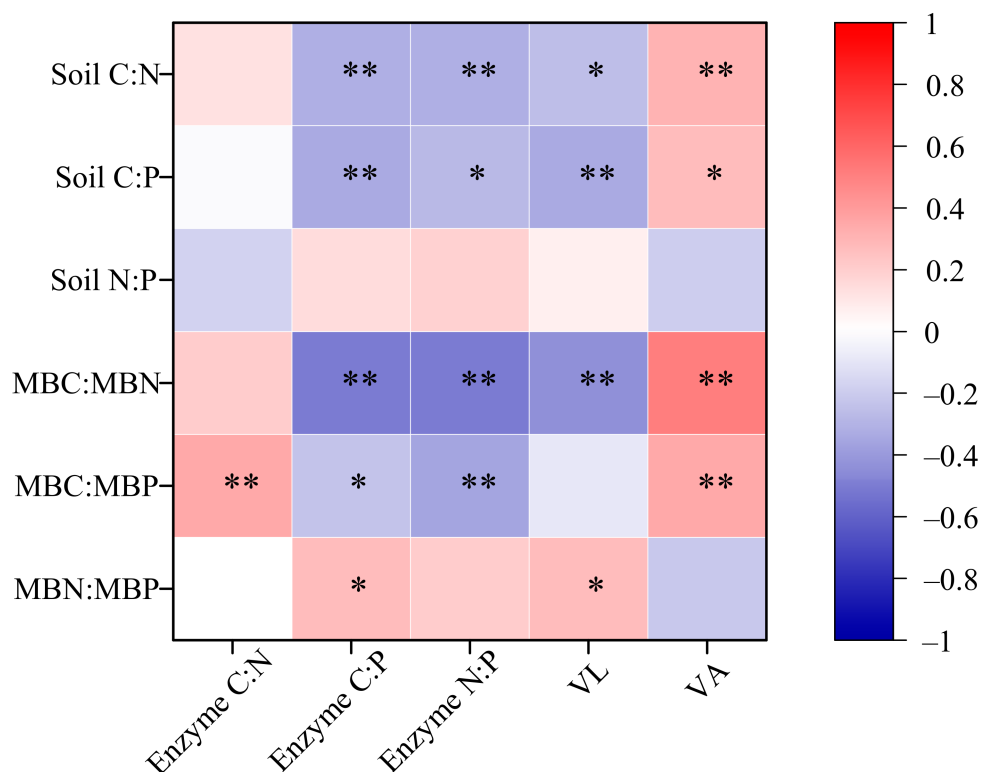


Figure 4a–c). By contrast, there was a highly significantly negative relationship between VA and VL among different treatments ( $p < 0.0001$ ; Figure 4d).



**Figure 4.** (a–d) Stoichiometric correlations among C-, N-, and P-acquiring enzymes within aggregates of different treatments.

The correlation heat map showed that the enzyme C:N and enzyme C:P ratios were highly significantly positively linked to MBC:MBP and MBN:MBP ratios, respectively ( $p < 0.01$ ), whereas enzyme C:P and enzyme N:P ratios were highly significantly negatively linked to soil C:N, C:P, MBC:MBN, and MBC:MBP ratios, and VL was significantly positively related to the MBN:MBP ratio ( $p < 0.05$ ), yet significantly adversely associated with soil C:N, C:P, and MBC:MBN ratios. Furthermore, VA was markedly favorably associated with soil C:N, C:P, MBC:MBN, and MBC:MBP ratios ( $p < 0.05$ ; Figure 5).



**Figure 5.** Heat map of the correlations among EES and soil nutrients and microbial biomass stoichiometry ratios within soil aggregates of different treatments. Enzyme C:N,  $\ln(\text{BG} + \text{CB} + \text{XYL})$ :  $\ln(\text{LAP} + \text{NAG})$ ; Enzyme C:P,  $\ln(\text{BG} + \text{CB} + \text{XYL})$ :  $\ln(\text{ALP})$ ; Enzyme N:P,  $\ln(\text{LAP} + \text{NAG})$ :  $\ln(\text{ALP})$ ; VL, vector length; VA, vector angle( $^{\circ}$ ). Soil C:N, soil carbon to nitrogen ratio; Soil C:P, soil carbon to phosphorus ratio; Soil N:P, soil nitrogen to phosphorus ratio; MBC:MBN, microbial biomass carbon to microbial biomass nitrogen ratio; MBC:MBP, microbial biomass carbon to microbial biomass phosphorus ratio; MBN:MBP, microbial biomass nitrogen to microbial biomass phosphorus ratio. \*  $p < 0.05$ , \*\*  $p < 0.01$ .

### 3.3. Factors Influencing Soil EEA and EES

Variance partitioning analysis (VPA) of EEA indicated that 77.7% of the variation was explained by a combination of soil physicochemical and microbial properties. Specifically, 43.0% of EEA variation was explainable by the co-effects of soil physicochemical and microbial properties (Figure 6A), whereas individual influences by soil physicochemical and microbial properties explained only 20.4% and 14.3% of EEA variation, respectively (Figure 6A). Among the examined soil physicochemical and microbial variables, 13 factors were significantly related to EEA variation, and forward selection in the RDA indicated that EEA variation was primarily driven by AP, MBC, soil C:N, MBN:MBP, soil N:P, and  $\text{NO}_3^-$ -N ( $p < 0.05$ , Figure 6B).

VPA of EES indicated that 65.8% of the variation was explained by a combination of soil physicochemical and microbial characteristics. Specifically, 34.1% of the EES variation was explainable by the co-effects by soil physicochemical and microbial properties (Figure 7A), whereas their individual effects explained only 14.8% and 17% of the EES variation, respectively (Figure 7A). Among soil physicochemical and microbial variables, 13 were significantly related to EES variation, and forward selection in the RDA indicated that EES variation was primarily driven by AP, MBC:MBN, TN, soil C:N, MBC, and MBN:MBP ( $p < 0.05$ , Figure 7B).

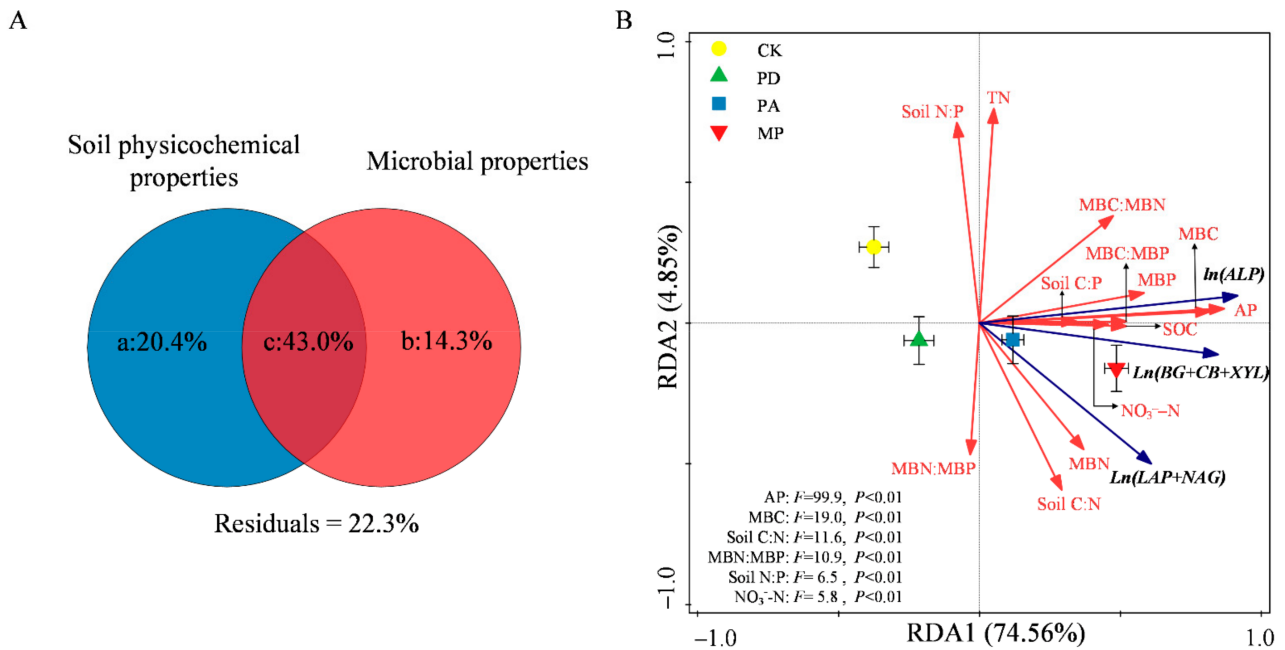


**Figure 6.** Variance partitioning analysis (VPA) for soil physicochemical and microbial characteristics on EEA (A). RDA was used to confirm the explanatory variables of different soil physicochemical and microbial properties on EEA (B). SOC, soil organic carbon; TN, total nitrogen; TP, total phosphorus;  $\text{NO}_3^-$ -N, nitrate nitrogen; AP, available phosphorus; Soil C:N, soil carbon to nitrogen ratio; Soil C:P, soil carbon to phosphorus ratio; Soil N:P, soil nitrogen to phosphorus ratio; MBC, microbial biomass carbon; MBN, microbial biomass nitrogen; MBP, microbial biomass phosphorus; MBC:MBN, microbial biomass carbon to microbial biomass nitrogen ratio; MBC:MBP, microbial biomass carbon to microbial biomass phosphorus ratio; MBN:MBP, microbial biomass nitrogen to microbial biomass phosphorus ratio.

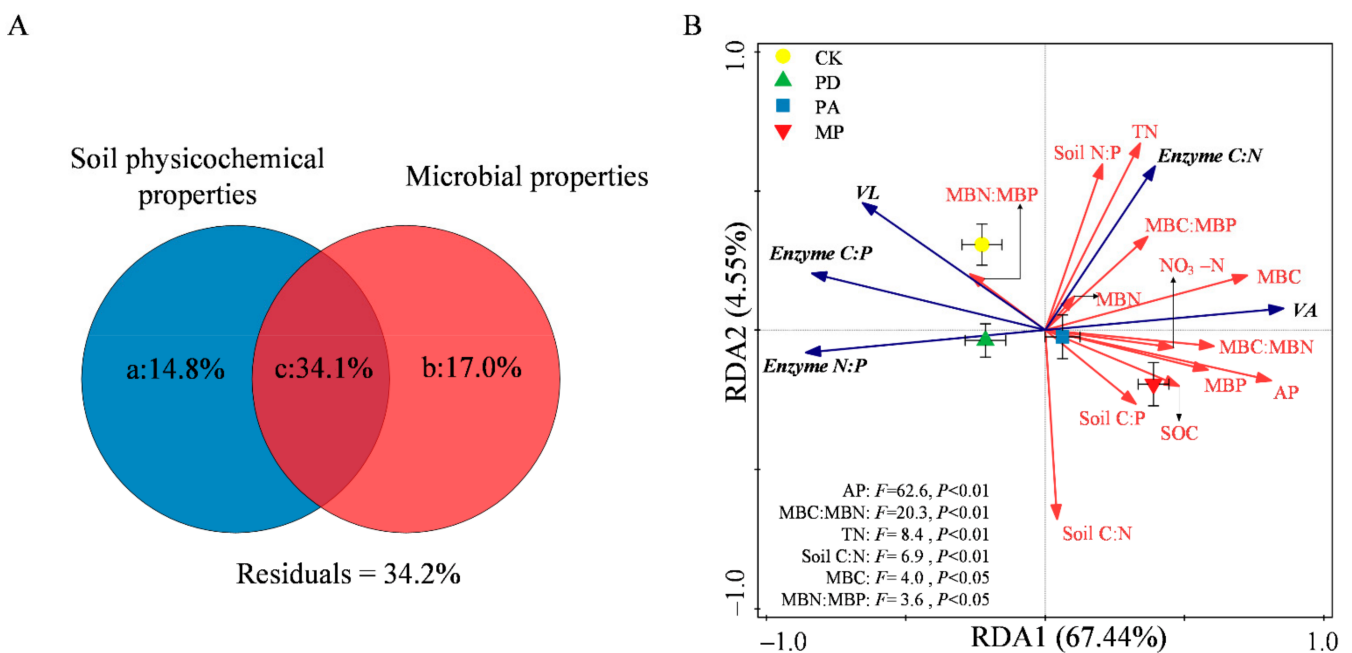


**Figure 7.** Variance partitioning analysis (VPA) of soil physicochemical and microbial characteristics on EES (A). RDA was used to confirm the explanatory variables of different soil physicochemical and microbial properties on EES (B). Enzyme C:N,  $\ln(\text{BG} + \text{CB} + \text{XYL})$ ;  $\ln(\text{LAP} + \text{NAG})$ ; enzyme C:P,  $\ln(\text{BG} + \text{CB} + \text{XYL})$ ;  $\ln(\text{ALP})$ ; enzyme N:P,  $\ln(\text{LAP} + \text{NAG})$ ;  $\ln(\text{ALP})$ ; VL, vector length; VA, vector angle( $^\circ$ ).

We used SEM analysis to further quantify the influences from complex soil nutrient, microbial biomass, and nutrient and microbial biomass stoichiometry on EEA and EES. The results showed there are direct or indirect relationships between various properties and EEA and EES (Figure 8a). EEA was directly and positively affected by nutrient stoichiometry and microbial biomass (effects were 0.22 and 0.75, respectively). However, EES was directly and negatively influenced by soil nutrient, microbial biomass stoichiometry, and EEA (effects were  $-0.19$ ,  $-0.30$ , and  $-0.61$ , respectively). Overall, microbial biomass had a positive and the strongest overall effect on EEA (0.73), while EES had the greatest negative overall effect by EEA ( $-0.61$ , Figure 8b).

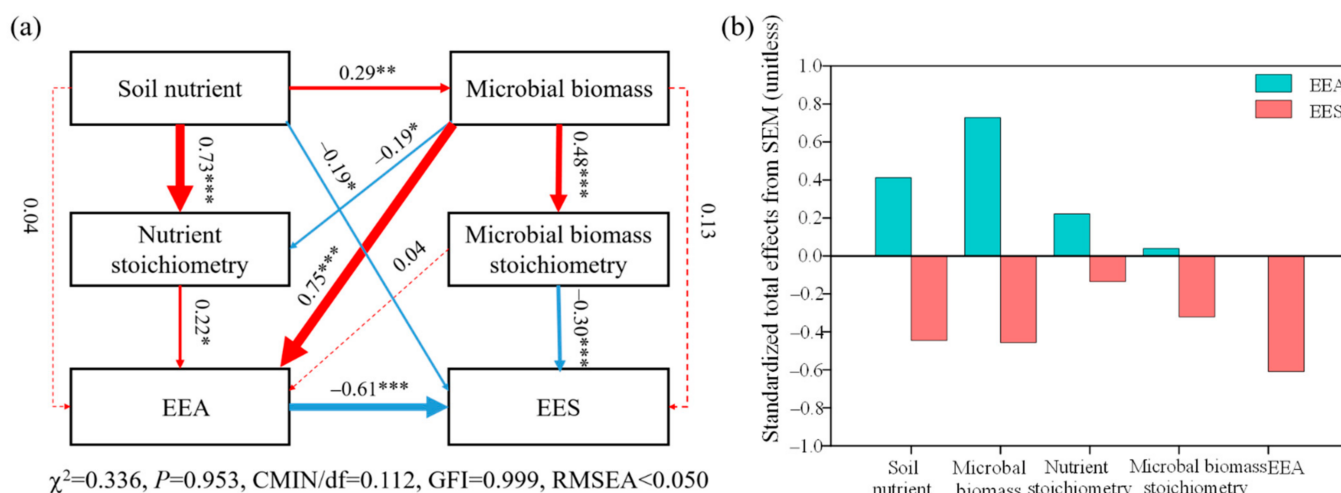


**Figure 8.** (a) SEM based on EEA and EES. Goodness-of-fit statistics for the model are exhibited below the models. (b) Standardized total effects on EEA and EES exported by SEM. Soil nutrient was calculated as a weight sum of SOM, TN,  $\text{NO}_3^-$ -N, and AP. Microbial biomass was calculated as a weight sum of MBC, MBN, and MBP. Nutrient stoichiometry was calculated as a weight sum of soil C:N, soil C:P, and soil N:P ratios. Microbial biomass stoichiometry were calculated as a weight sum of MBC:MBN, MBC:MBP, and MBN:MBP ratios. EEA was calculated as a weight sum of C-, N-, and P-acquiring enzyme activities. EES was calculated as a weight sum of enzyme C:N, enzyme C:P, and enzyme N:P ratios. Blue and red arrows denote negative and positive effects, respectively. Arrow widths are proportional to the magnitude of the path coefficients. Numbers on arrows are standardized direct effects. Continuous and dashed arrows mean significant and insignificant correlations, respectively. \*  $p < 0.05$ , \*\*  $p < 0.01$ , \*\*\*  $p < 0.001$ .

## 4. Discussion

### 4.1. Influences from $\text{N}_2$ -Fixer Tree Species on Soil EEA in Aggregates

Soil EEA can be sensitive to both natural and anthropogenic disturbances and therefore is a significant predictor for evaluating soil biological activity and soil nutrient efficiency to guide forest and environmental stress management practices [58,59]. The findings of this study indicated that for all aggregate sizes, C-, N-, and P-acquiring activities increased by different magnitudes compared to CK after introducing  $\text{N}_2$ -fixer tree species, particularly in MP (Figure 1), supporting the hypothesis (1) made earlier, which indicates that introducing  $\text{N}_2$ -fixer tree species can promote the cycles and transformation of C, N, and P within the soil aggregates (Figure 1). These findings may be attributed to the fact that introducing  $\text{N}_2$ -fixing tree species altered the composition of aboveground vegetation and stand structure, increasing biodiversity and forest productivity [38,60], which directly affected the quality and quantity of litterfall in the soil surface layer [61]. Litterfall is an essential source of SOM and a reactive substrate for soil microorganisms, thereby causing variations of the structure and function for soil microbial communities [62–64] and ultimately altering soil EEA. Thus, soil quality is an important factor influencing EEA, as the majority of soil enzymes show maximum activity over given ranges of N, P, and pH [65], which is consistent with previous

findings that  $N_2$ -fixer tree species may improve effectiveness of N in soil through symbiotic N fixation with microorganisms, contributing to improved N limitation [10] and enhancing other essential nutrients and overall soil quality [6,66]. Our results provide evidence that soil physicochemical and microbial properties are two major factors accounting for ~80% of variation in soil EEA within aggregates (Figure 6A). In addition, microbial properties take more responsibilities to influence changes in EEA compared to soil properties (Figure 8b). Most importantly, consistent with hypothesis (2), we found that EEA was significantly related to soil properties (such as AP, soil C:N, soil N:P, and  $NO_3^-$ -N) and microbial properties (such as MBC and MBN:MBP) (Figure 6B). This may be due to the fact that soil nutrients and microbes are naturally associated with the production of enzymes [67]. The significance of soil nutrients and microbial biomass to explain changes of EEA and EES was partially accepted by the research on the recovered ecosystem in Chinese Loess Plateau [68]. Furthermore, the litterfall of  $N_2$ -fixer tree species is enriched with C and N, which are easily broken down by bacteria and fungi, releasing more nutrients to return to the surface soil [69] and enabling soil microorganisms to synthesize C- and N-acquiring enzymes more rapidly [70].

Aggregates are the fundamental units of soil structure, which supply an important site for material–energy transformation and metabolism in the soil [22]. Soil enzymes are the most active part of the soil, and EEA distribution varies among aggregate sizes [71]. We found that in addition to treatment, aggregate size had a significant effect on changes in C-, N-, and P-acquiring enzyme activities (Figure 1). The values of REAI and REACI were >1 for more than 80% of aggregates with small particle sizes (Table 2), indicating that small aggregates played a protective role against soil enzymes, which is contrary to the findings of Zhong et al. [72]. This result occurred partly because small aggregates are the first to form (as large aggregates form through the adherence of small aggregates) and have more stable organic matter and substrates, such that enzymes are physically protected from degradation and denaturation deactivation by adsorption or colloid binding [73,74]. In addition, prior studies have shown that smaller aggregates have larger specific surface area and will adsorb more soil organic matter, providing more material for enzyme reactions and leading to higher EEA [75]. Similarly, the smaller pore sizes of small aggregates protect microorganisms from contact by external microorganisms, thereby providing physical protection to microorganisms, organic matter, and enzymes within the aggregates [76]. We detected an interaction on REAI and REACI of surface soil among treatment and aggregate size, which were >1 in most aggregates in MP, unlike those in CK, PD, and PA stands (Table 2), indicating that soil aggregates in MP plots were the most effective for protecting soil enzymes. As previous studies have shown, symbiotic N fixation by microorganisms associated with introducing  $N_2$ -fixer tree species, particularly mixing of  $N_2$ -fixer tree species, influences plant growth and soil microbial communities, and thus soil EEA through bottom-up effects [77,78].

#### 4.2. Influences from $N_2$ -Fixer Tree Species on Microbiological Nutrient Limitations, as Indicated by EES in Aggregates

EES has been broadly used to predict relevant requirements for metabolism of microorganisms and provides insight into the growth and metabolic status of microorganisms limited by C, N, and P [9,79,80]. In the research, the soil enzyme C:N ratio was 1.11 (lower than the global level of 1.41), and the enzyme N:P ratio was 1.08 (higher than the global level of 0.44) [79]. These findings indicated that microorganisms of the soil were seriously limited by N. Furthermore, the soil enzyme C:P ratio of 1.20 was higher than the global level of 0.62 [79], suggesting that soil microorganisms in the study were more restricted by C than P. Next, we also found that the soil enzyme C:N:P ratio in our study area was 1.20:1.09:1, which deviated from the global ratio (1:1:1) [79]. The soil enzyme C:N:P ratios in our study area were 1.23:1.10:1 in CK, 1.23:1.11:1 in PD, 1.19:1.08:1 in PA, and 1.16:1.05:1 in MP (Figure 2), suggesting lower P-acquiring EEA than C- or N-acquiring EEA, and higher C-acquiring EEA than N- or P-acquiring EEA. Therefore, we infer that soil EES in all

stands in the region depends on soil resource effectiveness rather than homeostasis and is mainly co-limited by C and N. The VA was  $<45^\circ$  in all four stands (Figure 3b) for all aggregates except  $<0.25$  mm aggregates in MP, also suggesting that microorganisms were generally limited by N; however, MP alleviated microbial N limitation to some extent relative to other stands [56] (Figure 3b), which was consistent with hypothesis (1). N limitation aggravated the degraded karst landscape restoration, leading to the secretion of more N- than P-acquiring enzymes through microbial metabolism [81]. Further, VL decreased by introducing N<sub>2</sub>-fixer tree species, particularly within MP, indicating that microorganisms were less limited by C in these plots.

In our study, introducing N<sub>2</sub>-fixer tree species, particularly mixing of two N<sub>2</sub>-fixer species, increased soil N availability, which, together with the increased soil organic matter (Table S2), led to an increase in C- and N- acquiring EEA [82], in turn enhancing C and N acquisition by soil microorganisms. These added soil C and N contents were available to microbial metabolism and biomass accumulation in order to gradually alleviate microbial limitation by C and N [66,83]. Our VPA results show that EES was mainly influenced by the interaction between soil physicochemical and microbial properties (Figure 7A). Furthermore, consistent with hypothesis (2), AP, MBC: MBN, TN, soil C:N, MBC, and MBN:MBP were all significant drivers of EES variation (Figure 7B). A possible explanation is that different N<sub>2</sub>-fixing tree stands can affect soil moisture, temperature, SOC, and nutrient cycling [9,68,84], leading to dramatic changes in soil microbial metabolism, and ultimately affecting soil EES [80,85]. In addition, soil properties and microbial properties directly and indirectly regulate EEA and thus EES (Figure 8a), which further demonstrates that introducing N<sub>2</sub>-fixer tree species directly affected the soil resource status, causing changes in soil EEA and EES, and ultimately characterizing the resources limited state of soil microbial metabolism.

We also found a negative correlation between VL (microbial C limitation) and VA (microbial N limitation) (Figure 4), suggesting that soil microbial communities steadily maintained an internal nutrient balance and other nutrient metabolism after introducing N<sub>2</sub>-fixer tree species [86]. The findings of our study showed that enzyme C:P and enzyme N:P ratios were markedly negatively associated with both soil C:N and soil C:P ratios (Figure 5), perhaps because soil nutrient stoichiometry ratios powerfully effect the composition and metabolic activity in microbial communities [9], ultimately affecting soil EES. The utilization of microbial nutrient resources by soil enzymes reflects soil total microbial biomass, which in reverse reflects the paths related to soil C, N, and P cycles [87]. We also found the significant relationships among EES and most microbial biomass stoichiometry ratios (Figure 5), reflecting the importance of microbial biomass stoichiometry ratios as a tool for predicting ecosystem stability and nutrient cycling status, consisting with the findings of Xu et al. [8]. Microbial biomass stoichiometry ratios mostly rest with soil nutrients availability, which can regulate microbial physiological metabolism, as ultimately reflected in soil enzyme secretions [85]. Meanwhile, VL and VA were also markedly linked to most of the nutrient and microbial biomass stoichiometry ratios (Figure 5), indicating that nutrient and microbial biomass stoichiometry ratios have a strong influence on microbial nutrient acquisition. This influence may be caused by microorganisms maintaining the elemental stoichiometric balance and homeostasis and by differential supply of soil nutrients among different treatments [9,88]. Thus, our findings confirm that the cultivation of N<sub>2</sub>-fixer plants improves soil N effectiveness and alleviates N limitation of soil microorganisms to some extent [86]. Therefore, we infer that after introducing N<sub>2</sub>-fixer tree species in our study area, the soil EES of different tree species depended on the effectiveness of soil resources rather than homeostasis, emphasizing that an imbalance in soil nutrient availability significantly impacted microbial access to C, N, and P nutrients.

The MBC:MBN ratio characterizes relative nutrient limitation, with higher or lower values indicating greater C or N limitation, respectively [84]. Our results suggested that MBC:MBN ratio was a significant driver of soil EES variation (Figure 7B). To acclimatize to C and N limitation, soil microbes tend to produce more C- and N-acquiring enzymes [81],

leading to the significant and negative correlations among the MBC:MBN ratio and enzyme C:P and enzyme N:P ratios (Figure 5). This study area is located in a degraded karst landscape with an unstable soil nutrient cycle, resulting in low nutrient content available to soil microbes, prolonging the period of time required to restore the karst ecosystem to reach a state of nutrient balance.

## 5. Conclusions

We evaluated EEA and EES within soil aggregates to study microbial resource limitations under different N<sub>2</sub>-fixer tree species planting patterns in degraded karst landscape. Microbial nutrient metabolism was co-limited by C and N, providing insight into microbial biomass responses to nutrient limitations. We also found that aggregate structure had important effects on soil EEA, such that small aggregate particles are more protective of soil enzymes than large aggregate particles. PD, PA, and MP stands (particularly MP stand) further alleviated but did not remove soil microbial C and N limitations of this degraded karst ecosystem. Thus, our results demonstrate the importance of introducing N<sub>2</sub>-fixer tree species, particularly mixed *Dalbergia odorifera* and *Acrocarpus fraxinifolius* trees, to restore severely degraded karst soils. These findings highlight the potential of coupling of EEA and EES to indicate resource limitations of soil microorganisms and nutrient cycles during vegetation restoration in degraded karst ecosystems. Therefore, we suggest that it is necessary to improve fertilization management to increase the exchange sites of nutrients, so as to improve nutrient availability, maintain the structure and fertility of degraded karst soils, and realize vegetation restoration and sustainable utilization of soils in karst ecosystems of southwest China.

**Supplementary Materials:** The following supporting information can be downloaded at: <https://www.mdpi.com/article/10.3390/f13101701/s1>, Table S1: Table S1 Basic information of soil C-, N- and P-acquiring enzymes substrate; Table S2: Characteristics of soils from different treatments: results for aggregate fractions (mean ± standard error, n = 5).

**Author Contributions:** Conceptualization, X.S. and Y.Y.; methodology, X.S. and Y.Y.; software, W.Z. and G.G.; validation, Y.W. and W.S.; formal analysis, Y.Y.; investigation, J.Y. and G.G.; resources, X.H. and Y.Y.; data curation, X.S.; writing—original draft preparation, X.S.; writing—review and editing, X.S. and G.G.; visualization, J.Y. and W.Z.; supervision, Y.W., W.S. and Y.Y.; project administration, X.H. and Y.Y.; funding acquisition, X.H. and Y.Y. All authors have read and agreed to the published version of the manuscript.

**Funding:** This research was jointly funded by the National Natural Science Foundation of China (Nos. 31960240 and 32171755), the Guangxi Natural Science Foundation (Nos. 2019GXNSFAA185023) and the scientific research capacity building project for Youyiguan Forest Ecosystem Observation and Research Station of Guangxi under Grant No. 2203513003.

**Data Availability Statement:** Not applicable.

**Acknowledgments:** The authors would like to thank the Guangxi Forest Ecology and Conservation Key Laboratory and the State Key Laboratory of Conservation and Utilization of Subtropical Agro-Bioresources of Guangxi University for their support in processing our soil properties. We would also like to thank the International Center for Bamboo and Rattan Research in Beijing for their technical guidance in measuring soil enzymes.

**Conflicts of Interest:** The authors declare no conflict of interest.

## References

1. Tapia-Torres, Y.; Elser, J.J.; Souza, V.; García-Oliva, F. Ecoenzymatic stoichiometry at the extremes: How microbes cope in an ultra-oligotrophic desert soil. *Soil Biol. Biochem.* **2015**, *87*, 34–42. [[CrossRef](#)]
2. Jing, X.; Yang, X.; Ren, F.; Zhou, H.; Zhu, B.; He, J. Neutral effect of nitrogen addition and negative effect of phosphorus addition on topsoil extracellular enzymatic activities in an alpine grassland ecosystem. *Appl. Soil Ecol.* **2016**, *107*, 205–213. [[CrossRef](#)]
3. Jian, S.; Li, J.; Chen, J.; Wang, G.; Mayes, M.A.; Dzantor, K.E.; Hui, D.; Luo, Y. Soil extracellular enzyme activities, soil carbon and nitrogen storage under nitrogen fertilization: A meta-analysis. *Soil Biol. Biochem.* **2016**, *101*, 32–43. [[CrossRef](#)]

4. Chen, J.; Luo, Y.; Li, J.; Zhou, X.; Cao, J.; Wang, R.W.; Wang, Y.; Shelton, S.; Jin, Z.; Walker, L.M.; et al. Costimulation of soil glycosidase activity and soil respiration by nitrogen addition. *Glob. Chang. Biol.* **2017**, *23*, 1328–1337. [[CrossRef](#)]
5. Cui, Y.; Bing, H.; Fang, L.; Jiang, M.; Shen, G.; Yu, J.; Wang, X.; Zhu, H.; Wu, Y.; Zhang, X. Extracellular enzyme stoichiometry reveals the carbon and phosphorus limitations of microbial metabolisms in the rhizosphere and bulk soils in alpine ecosystems. *Plant Soil* **2021**, *458*, 7–20. [[CrossRef](#)]
6. Dong, C.; Wang, W.; Liu, H.; Xu, X.; Zeng, H. Temperate grassland shifted from nitrogen to phosphorus limitation induced by degradation and nitrogen deposition: Evidence from soil extracellular enzyme stoichiometry. *Ecol. Indic.* **2019**, *101*, 453–464. [[CrossRef](#)]
7. Sinsabaugh, R.L.; Lauber, C.L.; Weintraub, M.N.; Ahmed, B.; Allison, S.D.; Crenshaw, C.; Contosta, A.R.; Cusack, D.; Frey, S.; Gallo, M.E.; et al. Stoichiometry of soil enzyme activity at global scale. *Ecol. Lett.* **2008**, *11*, 1252–1264. [[CrossRef](#)]
8. Xu, Z.; Yu, G.; Zhang, X.; He, N.; Wang, Q.; Wang, S.; Wang, R.; Zhao, N.; Jia, Y.; Wang, C. Soil enzyme activity and stoichiometry in forest ecosystems along the North-South Transect in eastern China (NSTEC). *Soil Biol. Biochem.* **2017**, *104*, 152–163. [[CrossRef](#)]
9. Cui, Y.; Fang, L.; Guo, X.; Wang, X.; Zhang, Y.; Li, P.; Zhang, X. Ecoenzymatic stoichiometry and microbial nutrient limitation in rhizosphere soil in the arid area of the northern Loess Plateau, China. *Soil Biol. Biochem.* **2018**, *116*, 11–21. [[CrossRef](#)]
10. Chen, H.; Li, D.; Zhao, J.; Zhang, W.; Xiao, K.; Wang, K. Nitrogen addition aggravates microbial carbon limitation: Evidence from ecoenzymatic stoichiometry. *Geoderma* **2018**, *329*, 61–64. [[CrossRef](#)]
11. Zungu, N.S.; Egbewale, S.O.; Olaniran, A.O.; Pérez-Fernández, M.; Magadlela, A. Soil nutrition, microbial composition and associated soil enzyme activities in KwaZulu-Natal grasslands and savannah ecosystems soils. *Appl. Soil Ecol.* **2020**, *155*, 103663. [[CrossRef](#)]
12. Deltedesco, E.; Keiblinger, K.M.; Piepho, H.; Antonielli, L.; Pötsch, E.M.; Zechmeister-Boltenstern, S.; Gorfer, M. Soil microbial community structure and function mainly respond to indirect effects in a multifactorial climate manipulation experiment. *Soil Biol. Biochem.* **2020**, *142*, 107704. [[CrossRef](#)]
13. Zheng, T.; Liang, C.; Xie, H.; Zhao, J.; Yan, E.; Zhou, X.; Bao, X. Rhizosphere effects on soil microbial community structure and enzyme activity in a successional subtropical forest. *FEMS Microbiol. Ecol.* **2019**, *95*, fiz043. [[CrossRef](#)] [[PubMed](#)]
14. Kooch, Y.; Noghre, N. Nutrient cycling and soil-related processes under different land covers of semi-arid rangeland ecosystems in northern Iran. *Catena* **2020**, *193*, 104621. [[CrossRef](#)]
15. Wang, H.; Wu, J.; Li, G.; Yan, L. Changes in soil carbon fractions and enzyme activities under different vegetation types of the northern Loess Plateau. *Ecol. Evol.* **2020**, *10*, 12211–12223. [[CrossRef](#)] [[PubMed](#)]
16. Wang, L.; Pang, X.; Li, N.; Qi, K.; Huang, J.; Yin, C. Effects of vegetation type, fine and coarse roots on soil microbial communities and enzyme activities in eastern Tibetan plateau. *Catena* **2020**, *194*, 104694. [[CrossRef](#)]
17. Zheng, H.; Chen, Y.; Liu, Y.; Heděnc, P.; Peng, Y.; Xu, Z.; Tan, B.; Zhang, L.; Guo, L.; Wang, L. Effects of litter quality diminish and effects of vegetation type develop during litter decomposition of two shrub species in an alpine treeline ecotone. *Ecosystems* **2021**, *24*, 197–210. [[CrossRef](#)]
18. Luo, D.; Cheng, R.; Liu, S.; Shi, Z.; Feng, Q. Responses of soil microbial community composition and enzyme activities to land-use change in the Eastern Tibetan Plateau, China. *Forests* **2020**, *11*, 483. [[CrossRef](#)]
19. Sun, Y.; Luo, C.; Jiang, L.; Song, M.; Zhang, D.; Li, J.; Li, Y.; Ostle, N.J.; Zhang, G. Land-use changes alter soil bacterial composition and diversity in tropical forest soil in China. *Sci. Total Environ.* **2020**, *712*, 136526. [[CrossRef](#)]
20. Mangalassery, S.; Sjögersten, S.; Sparkes, D.L.; Sturrock, C.J.; Mooney, S.J. The effect of soil aggregate size on pore structure and its consequence on an emission of greenhouse gases. *Soil Till. Res.* **2013**, *132*, 39–46. [[CrossRef](#)]
21. Ye, C.; Guo, Z.; Cai, C.; Wang, J.; Deng, J. Effect of water content, bulk density, and aggregate size on mechanical characteristics of Aquilts soil blocks and aggregates from subtropical China. *J. Soil Sediment.* **2017**, *17*, 210–219. [[CrossRef](#)]
22. Six, J.; Paustian, K. Aggregate-associated soil organic matter as an ecosystem property and a measurement tool. *Soil Biol. Biochem.* **2014**, *68*, A4–A9. [[CrossRef](#)]
23. Wei, X.; Huang, C.; Wei, N.; Zhao, H.; He, Y.; Wu, X. The impact of freeze–thaw cycles and soil moisture content at freezing on runoff and soil loss. *Land Degrad. Dev.* **2019**, *30*, 515–523. [[CrossRef](#)]
24. Okolo, C.C.; Gebresamuel, G.; Zenebe, A.; Haile, M.; Eze, P.N. Accumulation of organic carbon in various soil aggregate sizes under different land use systems in a semi-arid environment. *Agric. Ecosyst. Environ.* **2020**, *297*, 106924. [[CrossRef](#)]
25. Fang, X.; Zhou, G.; Li, Y.; Liu, S.; Chu, G.; Xu, Z.; Liu, J. Warming effects on biomass and composition of microbial communities and enzyme activities within soil aggregates in subtropical forest. *Biol. Fert. Soils* **2016**, *52*, 353–365. [[CrossRef](#)]
26. Wang, L.; Luo, X.; Liao, H.; Chen, W.; Wei, D.; Cai, P.; Huang, Q. Ureolytic microbial community is modulated by fertilization regimes and particle-size fractions in a Black soil of Northeastern China. *Soil Biol. Biochem.* **2018**, *116*, 171–178. [[CrossRef](#)]
27. Lu, J.; Zheng, F.; Li, G.; Bian, F.; An, J. The effects of raindrop impact and runoff detachment on hillslope soil erosion and soil aggregate loss in the Mollisol region of Northeast China. *Soil Tillage Res.* **2016**, *161*, 79–85. [[CrossRef](#)]
28. Jiang, Z.; Lian, Y.; Qin, X. Rocky desertification in Southwest China: Impacts, causes, and restoration. *Earth-Sci. Rev.* **2014**, *132*, 1–12. [[CrossRef](#)]
29. Lu, Z.; Wang, P.; Ou, H.; Wei, S.; Wu, L.; Jiang, Y.; Wang, R.; Liu, X.; Wang, Z.; Chen, L.; et al. Effects of different vegetation restoration on soil nutrients, enzyme activities, and microbial communities in degraded karst landscapes in southwest China. *For. Ecol. Manag.* **2022**, *508*, 120002. [[CrossRef](#)]



30. Liu, C.; Liu, Y.; Guo, K.; Zhao, H.; Qiao, X.; Wang, S.; Zhang, L.; Cai, X. Mixing litter from deciduous and evergreen trees enhances decomposition in a subtropical karst forest in southwestern China. *Soil Biol. Biochem.* **2016**, *101*, 44–54. [[CrossRef](#)]
31. Li, D.; Wen, L.; Yang, L.; Luo, P.; Xiao, K.; Chen, H.; Zhang, W.; He, X.; Chen, H.; Wang, K. Dynamics of soil organic carbon and nitrogen following agricultural abandonment in a karst region. *J. Geophys. Res. Biogeosciences* **2017**, *122*, 230–242. [[CrossRef](#)]
32. Zhang, W.; Zhao, J.; Pan, F.; Li, D.; Chen, H.; Wang, K. Changes in nitrogen and phosphorus limitation during secondary succession in a karst region in southwest China. *Plant Soil* **2015**, *391*, 77–91. [[CrossRef](#)]
33. Liu, X.; Zhang, W.; Wu, M.; Ye, Y.; Wang, K.; Li, D. Changes in soil nitrogen stocks following vegetation restoration in a typical karst catchment. *Land Degrad. Dev.* **2019**, *30*, 60–72. [[CrossRef](#)]
34. Hu, P.L.; Liu, S.J.; Ye, Y.Y.; Zhang, W.; Wang, K.L.; Su, Y.R. Effects of environmental factors on soil organic carbon under natural or managed vegetation restoration. *Land Degrad. Dev.* **2018**, *29*, 387–397. [[CrossRef](#)]
35. Guan, H.; Fan, J. Effects of vegetation restoration on soil quality in fragile karst ecosystems of southwest China. *PeerJ* **2020**, *8*, e9456. [[CrossRef](#)]
36. Turner, B.L.; Joseph Wright, S. The response of microbial biomass and hydrolytic enzymes to a decade of nitrogen, phosphorus, and potassium addition in a lowland tropical rain forest. *Biogeochemistry* **2014**, *117*, 115–130. [[CrossRef](#)]
37. Waithaisong, K.; Robin, A.; Martin, A.; Clairotte, M.; Villeneuve, M.; Deleporte, P.; Plassard, C. N-fixing tree species introduced in Eucalyptus forest modify soil organic P and low molecular weight organic acid pools. In Proceedings of the PSP5 2014-Facing Phosphorus Scarcity, Montpellier, France, 26–29 August 2014.
38. Ouyang, S.; Xiang, W.; Wang, X.; Xiao, W.; Chen, L.; Li, S.; Sun, H.; Deng, X.; Forrester, D.I.; Zeng, L.; et al. Effects of stand age, richness and density on productivity in subtropical forests in China. *J. Ecol.* **2019**, *107*, 2266–2277. [[CrossRef](#)]
39. Ouyang, S.; Xiang, W.; Gou, M.; Chen, L.; Lei, P.; Xiao, W.; Deng, X.; Zeng, L.; Li, J.; Zhang, T.; et al. Stability in subtropical forests: The role of tree species diversity, stand structure, environmental and socio-economic conditions. *Glob. Ecol. Biogeogr.* **2021**, *30*, 500–513. [[CrossRef](#)]
40. Xue, L.; Ren, H.; Li, S.; Leng, X.; Yao, X. Soil bacterial community structure and co-occurrence pattern during vegetation restoration in karst rocky desertification area. *Front. Microbiol.* **2017**, *8*, 2377. [[CrossRef](#)]
41. Li, D.; Wen, L.; Jiang, S.; Song, T.; Wang, K. Responses of soil nutrients and microbial communities to three restoration strategies in a karst area, southwest China. *J. Environ. Manag.* **2018**, *207*, 456–464. [[CrossRef](#)]
42. Wang, Y.; Dungait, J.A.J.; Xing, K.; Green, S.M.; Hartley, I.; Tu, C.; Quine, T.A.; Tian, J.; Kuzyakov, Y. Persistence of soil microbial function at the rock-soil interface in degraded karst topsoils. *Land Degrad. Dev.* **2019**, *31*, 251–265. [[CrossRef](#)]
43. Li, M.; You, Y.; Tan, X.; Wen, Y.; Yu, S.; Xiao, N.; Shen, W.; Huang, X. Mixture of N<sub>2</sub>-fixing tree species promotes organic phosphorus accumulation and transformation in topsoil aggregates in a degraded karst region of subtropical China. *Geoderma* **2022**, *413*, 115752. [[CrossRef](#)]
44. Schutter, M.E.; Dick, R.P. Microbial community profiles and activities among aggregates of winter fallow and cover-cropped soil. *Soil Sci. Soc. Am. J.* **2002**, *66*, 142–153. [[CrossRef](#)]
45. Guo, L.; Shen, J.; Li, B.; Li, Q.; Wang, C.; Guan, Y.; D’Acqui, L.P.; Luo, Y.; Tao, Q.; Xu, Q.; et al. Impacts of agricultural land use change on soil aggregate stability and physical protection of organic C. *Sci. Total Environ.* **2020**, *707*, 136049. [[CrossRef](#)] [[PubMed](#)]
46. Bremner, J.M. Nitrogen-total. In *Methods of Soil Analysis: Part 3 Chemical Methods*; Soil Science Society of America, Inc.: Madison, WI, USA; American Society of Agronomy, Inc.: Madison, WI, USA, 1996; Volume 5, pp. 1085–1121.
47. Murphy, J.; Riley, J.P. A modified single solution method for the determination of phosphate in natural waters. *Anal. Chim. Acta.* **1962**, *27*, 31–36. [[CrossRef](#)]
48. Olsen, S.R. *Estimation of Available Phosphorus in Soils by Extraction with Sodium Bicarbonate*; US Department of Agriculture: Washington, DC, USA, 1954.
49. Jenkinson, D.S.; Powlson, D.S. The effects of biocidal treatments on metabolism in soil—V: A method for measuring soil biomass. *Soil Biol. Biochem.* **1976**, *8*, 209–213. [[CrossRef](#)]
50. Brookes, P.C.; Powlson, D.S.; Jenkinson, D.S. Measurement of microbial biomass phosphorus in soil. *Soil Biol. Biochem.* **1982**, *14*, 319–329. [[CrossRef](#)]
51. Vance, E.D.; Brookes, P.C.; Jenkinson, D.S. An extraction method for measuring soil microbial biomass C. *Soil Biol. Biochem.* **1987**, *19*, 703–707. [[CrossRef](#)]
52. Saiya-Cork, K.R.; Sinsabaugh, R.L.; Zak, D.R. The effects of long term nitrogen deposition on extracellular enzyme activity in an *Acer saccharum* forest soil. *Soil Biol. Biochem.* **2002**, *34*, 1309–1315. [[CrossRef](#)]
53. Fairbanks, D.; Shepard, C.; Murphy, M.; Rasmussen, C.; Chorover, J.; Rich, V.; Gallery, R. Depth and topographic controls on microbial activity in a recently burned sub-alpine catchment. *Soil Biol. Biochem.* **2020**, *148*, 107844. [[CrossRef](#)]
54. He, L.; Lu, S.; Wang, C.; Mu, J.; Zhang, Y.; Wang, X. Changes in soil organic carbon fractions and enzyme activities in response to tillage practices in the Loess Plateau of China. *Soil Tillage Res.* **2021**, *209*, 104940. [[CrossRef](#)]
55. Fattet, M.; Fu, Y.; Ghestem, M.; Ma, W.; Foulonneau, M.; Nespoulous, J.; Le Bissonnais, Y.; Stokes, A. Effects of vegetation type on soil resistance to erosion: Relationship between aggregate stability and shear strength. *Catena* **2011**, *87*, 60–69. [[CrossRef](#)]
56. Moorhead, D.L.; Sinsabaugh, R.L.; Hill, B.H.; Weintraub, M.N. Vector analysis of ecoenzyme activities reveal constraints on coupled C, N and P dynamics. *Soil Biol. Biochem.* **2016**, *93*, 1–7. [[CrossRef](#)]
57. You, Y.; Wang, J.; Huang, X.; Tang, Z.; Liu, S.; Sun, O.J. Relating microbial community structure to functioning in forest soil organic carbon transformation and turnover. *Ecol. Evol.* **2014**, *4*, 633–647. [[CrossRef](#)] [[PubMed](#)]

58. Nannipieri, P.; Giagnoni, L.; Renella, G.; Puglisi, E.; Ceccanti, B.; Masciandaro, G.; Fornasier, F.; Moscatelli, M.C.; Marinari, S. Soil enzymology: Classical and molecular approaches. *Biol. Fert. Soils*. **2012**, *48*, 743–762. [\[CrossRef\]](#)
59. Muscolo, A.; Settineri, G.; Attinà, E. Early warning indicators of changes in soil ecosystem functioning. *Ecol. Indic.* **2015**, *48*, 542–549. [\[CrossRef\]](#)
60. Yao, X.; Li, Y.; Liao, L.; Sun, G.; Wang, H.; Ye, S. Enhancement of nutrient absorption and interspecific nitrogen transfer in a *Eucalyptus urophylla* × *eucalyptus grandis* and *Dalbergia odorifera* mixed plantation. *For. Ecol. Manag.* **2019**, *449*, 117465. [\[CrossRef\]](#)
61. Santos, F.M.; Balieiro, F.D.C.; Fontes, M.A.; Chaer, G.M. Understanding the enhanced litter decomposition of mixed-species plantations of *Eucalyptus* and *Acacia mangium*. *Plant Soil* **2018**, *423*, 141–155. [\[CrossRef\]](#)
62. Yang, J.; Xu, X.; Liu, M.; Xu, C.; Zhang, Y.; Luo, W.; Zhang, R.; Li, X.; Kiely, G.; Wang, K. Effects of “Grain for Green” program on soil hydrologic functions in karst landscapes, southwestern China. *Agric. Ecosyst. Environ.* **2017**, *247*, 120–129. [\[CrossRef\]](#)
63. Pan, F.; Zhang, W.; Liang, Y.; Liu, S.; Wang, K. Increased associated effects of topography and litter and soil nutrients on soil enzyme activities and microbial biomass along vegetation successions in karst ecosystem, southwestern China. *Environ. Sci. Pollut. Res.* **2018**, *25*, 16979–16990. [\[CrossRef\]](#)
64. Pereira, A.P.A.; Durrer, A.; Gumiere, T.; Gonçalves, J.L.M.; Robin, A.; Bouillet, J.; Wang, J.; Verma, J.P.; Singh, B.K.; Cardoso, E.J.B.N. Mixed *Eucalyptus* plantations induce changes in microbial communities and increase biological functions in the soil and litter layers. *For. Ecol. Manag.* **2019**, *433*, 332–342. [\[CrossRef\]](#)
65. Wei, L.; Razavi, B.S.; Wang, W.; Zhu, Z.; Liu, S.; Wu, J.; Kuzyakov, Y.; Ge, T. Labile carbon matters more than temperature for enzyme activity in paddy soil. *Soil Biol. Biochem.* **2019**, *135*, 134–143. [\[CrossRef\]](#)
66. Zhu, X.; Liu, M.; Kou, Y.; Liu, D.; Liu, Q.; Zhang, Z.; Jiang, Z.; Yin, H. Differential effects of N addition on the stoichiometry of microbes and extracellular enzymes in the rhizosphere and bulk soils of an alpine shrubland. *Plant Soil* **2020**, *449*, 285–301. [\[CrossRef\]](#)
67. Yang, Y.; Liang, C.; Wang, Y.; Cheng, H.; An, S.; Chang, S.X. Soil extracellular enzyme stoichiometry reflects the shift from P- to N-limitation of microorganisms with grassland restoration. *Soil Biol. Biochem.* **2020**, *149*, 107928. [\[CrossRef\]](#)
68. Zhang, W.; Xu, Y.; Gao, D.; Wang, X.; Liu, W.; Deng, J.; Han, X.; Yang, G.; Feng, Y.; Ren, G. Ecoenzymatic stoichiometry and nutrient dynamics along a revegetation chronosequence in the soils of abandoned land and *Robinia pseudoacacia* plantation on the Loess Plateau, China. *Soil Biol. Biochem.* **2019**, *134*, 1–14. [\[CrossRef\]](#)
69. Viketoft, M.; Bengtsson, J.; Sohlenius, B.; Berg, M.P.; Petchey, O.; Palmborg, C.; Huss-Danell, K. Long-term effects of plant diversity and composition on soil nematode communities in model grasslands. *Ecology* **2009**, *90*, 90–99. [\[CrossRef\]](#)
70. Innangi, M.; Niro, E.; D Ascoli, R.; Danise, T.; Proietti, P.; Nasini, L.; Regni, L.; Castaldi, S.; Fioretto, A. Effects of olive pomace amendment on soil enzyme activities. *Appl. Soil Ecol.* **2017**, *119*, 242–249. [\[CrossRef\]](#)
71. Han, S.; Delgado-Baquerizo, M.; Luo, X.; Liu, Y.; Van Nostrand, J.D.; Chen, W.; Zhou, J.; Huang, Q. Soil aggregate size-dependent relationships between microbial functional diversity and multifunctionality. *Soil Biol. Biochem.* **2021**, *154*, 108143. [\[CrossRef\]](#)
72. Zhong, X.L.; Li, J.T.; Li, X.J.; Ye, Y.C.; Liu, S.S.; Xu, G.L.; Ni, J. Early effect of soil aggregates on enzyme activities in a forest soil with simulated N deposition elevation. *Acta. Ecol. Sin.* **2015**, *35*, 1422–1433.
73. Liang, Q.; Chen, H.; Gong, Y.; Yang, H.; Fan, M.; Kuzyakov, Y. Effects of 15 years of manure and mineral fertilizers on enzyme activities in particle-size fractions in a North China Plain soil. *Eur. J. Soil Biol.* **2014**, *60*, 112–119. [\[CrossRef\]](#)
74. Zhang, Q.; Zhou, W.; Liang, G.; Sun, J.; Wang, X.; He, P. Distribution of soil nutrients, extracellular enzyme activities and microbial communities across particle-size fractions in a long-term fertilizer experiment. *Appl. Soil Ecol.* **2015**, *94*, 59–71. [\[CrossRef\]](#)
75. von Lützow, M.; Kögel-Knabner, I.; Ekschmitt, K.; Flessa, H.; Guggenberger, G.; Matzner, E.; Marschner, B. SOM fractionation methods: Relevance to functional pools and to stabilization mechanisms. *Soil Biol. Biochem.* **2007**, *39*, 2183–2207. [\[CrossRef\]](#)
76. Steffens, M.; Kölbl, A.; Schörk, E.; Gschrey, B.; Kögel-Knabner, I. Distribution of soil organic matter between fractions and aggregate size classes in grazed semiarid steppe soil profiles. *Plant Soil* **2011**, *338*, 63–81. [\[CrossRef\]](#)
77. Meena, V.S.; Meena, S.K.; Verma, J.P.; Kumar, A.; Aeron, A.; Mishra, P.K.; Bisht, J.K.; Pattanayak, A.; Naveed, M.; Dotaniya, M.L. Plant beneficial rhizospheric microorganism (PBRM) strategies to improve nutrients use efficiency: A review. *Ecol. Eng.* **2017**, *107*, 8–32.
78. Chen, J.; Shen, W.; Xu, H.; Li, Y.; Luo, T. The Composition of Nitrogen-Fixing Microorganisms Correlates With Soil Nitrogen Content During Reforestation: A Comparison Between Legume and Non-legume Plantations. *Front. Microbiol.* **2019**, *10*, 508. [\[CrossRef\]](#) [\[PubMed\]](#)
79. Sinsabaugh, R.L.; Hill, B.H.; Follstad Shah, J.J. Ecoenzymatic stoichiometry of microbial organic nutrient acquisition in soil and sediment. *Nature* **2009**, *462*, 795–798. [\[CrossRef\]](#) [\[PubMed\]](#)
80. Peng, X.; Wang, W. Stoichiometry of soil extracellular enzyme activity along a climatic transect in temperate grasslands of northern China. *Soil Biol. Biochem.* **2016**, *98*, 74–84.
81. Wang, J.; Wang, X.; Liu, G.; Wang, G.; Wu, Y.; Zhang, C. Fencing as an effective approach for restoration of alpine meadows: Evidence from nutrient limitation of soil microbes. *Geoderma* **2020**, *363*, 114148. [\[CrossRef\]](#)
82. Nasto, M.K.; Alvarez Clare, S.; Lekberg, Y.; Sullivan, B.W.; Townsend, A.R.; Cleveland, C.C. Interactions among nitrogen fixation and soil phosphorus acquisition strategies in lowland tropical rain forests. *Ecol. Lett.* **2014**, *17*, 1282–1289. [\[CrossRef\]](#)

83. Zhong, Z.; Zhang, X.; Wang, X.; Fu, S.; Wu, S.; Lu, X.; Ren, C.; Han, X.; Yang, G. Soil bacteria and fungi respond differently to plant diversity and plant family composition during the secondary succession of abandoned farmland on the Loess Plateau, China. *Plant Soil* **2020**, *448*, 183–200. [[CrossRef](#)]
84. Ren, C.; Chen, J.; Deng, J.; Zhao, F.; Han, X.; Yang, G.; Tong, X.; Feng, Y.; Shelton, S.; Ren, G. Response of microbial diversity to C:N:P stoichiometry in fine root and microbial biomass following afforestation. *Biol. Fert. Soils* **2017**, *53*, 457–468. [[CrossRef](#)]
85. Zhao, F.Z.; Ren, C.J.; Han, X.H.; Yang, G.H.; Wang, J.; Doughty, R. Changes of soil microbial and enzyme activities are linked to soil C, N and P stoichiometry in afforested ecosystems. *For. Ecol. Manag.* **2018**, *427*, 289–295. [[CrossRef](#)]
86. Xu, M.; Li, W.; Wang, J.; Zhu, Y.; Feng, Y.; Yang, G.; Zhang, W.; Han, X. Soil coenzymatic stoichiometry reveals microbial phosphorus limitation after vegetation restoration on the Loess Plateau, China. *Sci. Total Environ.* **2022**, *815*, 152918. [[CrossRef](#)]
87. Jia, X.; Zhong, Y.; Liu, J.; Zhu, G.; Shanguan, Z.; Yan, W. Effects of nitrogen enrichment on soil microbial characteristics: From biomass to enzyme activities. *Geoderma* **2020**, *366*, 114256. [[CrossRef](#)]
88. Cui, Y.; Fang, L.; Guo, X.; Han, F.; Ju, W.; Ye, L.; Wang, X.; Tan, W.; Zhang, X. Natural grassland as the optimal pattern of vegetation restoration in arid and semi-arid regions: Evidence from nutrient limitation of soil microbes. *Sci. Total Environ.* **2019**, *648*, 388–397. [[CrossRef](#)] [[PubMed](#)]